

Freezing of low energy excitations in charge density wave glasses

D. Starešinić,^{1,a)} S. V. Zaitsev-Zotov,² N. I. Baklanov,² and K. Biljaković¹

¹*Institute of Physics, P.O. Box 304, HR-10001 Zagreb, Croatia*

²*Institute of Radioengineering and Electronics, Russian Academy of Sciences, Mokhovaya 11, 103907 Moscow, Russia*

(Received 19 September 2007; accepted 14 January 2008; published online 3 March 2008)

Thermally stimulated discharge current measurements were performed to study slow relaxation processes in two canonical charge density wave systems $K_{0.3}MoO_3$ and $o-TaS_3$. Two relaxation processes were observed and characterized in each system, corroborating the results of dielectric spectroscopy. Our results are consistent with the scenario of the glass transition on the charge density wave superstructure level. In particular, the results directly prove the previously proposed criterion of charge density wave freezing based on the interplay of charge density wave pinning by impurities and screening by free carriers. In addition, we obtained new information on distribution of relaxation parameters, as well as on nonlinear dielectric response both below and above the threshold field for charge density wave sliding. © 2008 American Institute of Physics.

[DOI: [10.1063/1.2840358](https://doi.org/10.1063/1.2840358)]

I. INTRODUCTION

A charge density wave (CDW) is a spatially modulated condensate of conducting electrons accompanied with a slight lattice distortion which stabilizes at a finite temperature in metallic crystals with a quasi-one-dimensional Fermi surface.¹ At the CDW transition temperature T_p the gap opens at the Fermi level due to the new periodicity and the system becomes semiconducting.

Complex low energy dynamics of CDW systems, which include nonlinear conductivity above the threshold electric field as low as a few mV/cm, a giant low frequency dielectric constant as high as 10^8 , narrow and broadband noise in nonlinear regime, etc., result from spatiotemporal distortions of complex order parameter in interaction with random impurities and uncondensed electrons.² Extensive investigation of the dielectric response of CDW systems in a wide frequency and temperature range^{3,4} showed that qualitative changes in CDW dynamics take place at the finite temperature at which elastic, phase distortions of the CDW superstructure freeze due to the condensation of free carriers. At lower temperatures plastic distortions (topological defects) govern CDW dynamics.

As seen in dielectric spectroscopy, this freezing has all the characteristics of the glass transition observed in supercooled liquids,⁵ such as the activated slowing-down of high temperature (primary or α) relaxational process,⁶⁻⁹ but particularly the emergence of the low temperature (secondary or β) relaxational process from the high frequency wing of the α process upon cooling which becomes dominant¹⁰ below the glass transition temperature T_g . Moreover, at least in $o-TaS_3$ (Ref. 3) the temperature dependence of the characteristic relaxation time exhibits a critical slowing down, typical of the so-called fragile glasses.¹¹ In Fig. 1, the characteristic relaxation times of both processes in $K_{0.3}MoO_3$ and

$o-TaS_3$ from Refs. 3 and 4 are presented in the so-called Angell plot,¹¹ i.e., the Arrhenius plot in which the temperature is rescaled to T_g , being 23 K for $K_{0.3}MoO_3$ and 42 K for $o-TaS_3$.

The peculiarity of the CDW glass transition is that it occurs on the level of the CDW superstructure in a structurally ordered crystal. The disorder inherent to glasses comes from the interaction of CDW with random impurities, which destroy the long-range phase coherence and create domains of the correlated phase.¹² The disorder is manifested at the scale of micrometers, a typical domain size in CDW systems,^{13,14} instead of nanometers as in glasses. The interaction of domains is electrostatic in nature¹⁵ and its strength depends on the availability of free carriers to screen this long-range Coulomb interaction and thus enable domains to relax.¹⁶ Therefore, the inverse free carrier density (or average volume per free carrier) has the role of the generalized viscosity for CDW. The freezing occurs when the density of free carriers excited over the CDW gap is too low to screen the domains efficiently. It may be quantified as the density at which there is less than one free carrier per domain, based on the indirect evidence inferred from the dielectric spectroscopy results.^{3,4} As the mechanism of glassy behavior in CDW based on pinning and screening¹⁶⁻¹⁹ is rather well-founded, the understanding of glass transition in CDW might help in understanding the glass transition in general. However, the concept of the mesoscopic glass of the superstructure has not been easy to accept either in CDW or in glass community and we are working on a better understanding and presentation.

This paper reports the results of the thermally stimulated depolarization²⁰ (TSD) method applied to two canonical CDW systems: $K_{0.3}MoO_3$ and $o-TaS_3$. TSD is used for the investigation of very slow dielectric relaxation processes in highly resistive and polarizable systems, such as CDW systems at low temperature, via the study of thermal relaxation effects. In this respect, TSD is a complementary method to

^{a)}Electronic mail: damirs@ifs.hr.

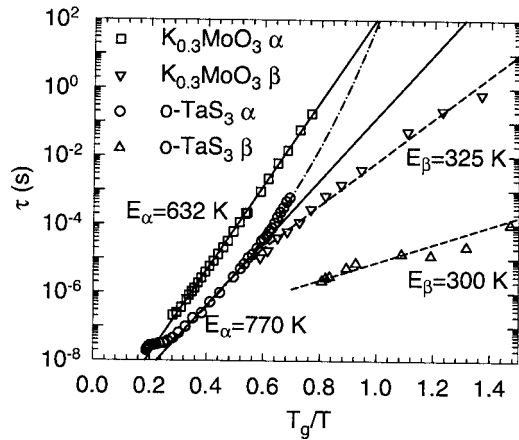


FIG. 1. Characteristic relaxation times of the α and β processes observed in $K_{0.3}MoO_3$ and $o-TaS_3$ as the function of the temperature normalized to the glass transition temperature T_g which is 23 K for $K_{0.3}MoO_3$ and 42 K for $o-TaS_3$. Full lines represent the fits to the activated dependence [Eq. (1)] of $\tau(T)$ for the α process, and dashed lines for the β process. Dash-dotted line is the fit to the Vogel-Fulcher temperature dependence $\tau(T) = \tau_0 \exp(E_{act}/(T-T_0))$ for the α process in $o-TaS_3$.

dielectric spectroscopy. In many electret materials such as polymers, dipolar glasses, and semiconductors with impurities the TSD current spectra are used to observe different relaxation processes and to determine related microscopic parameters.²⁰ Our results confirm the existence of two relaxation processes in both $o-TaS_3$ and $K_{0.3}MoO_3$. They also confirm directly the proposed freezing criterion,^{3,4} as the results show that the volume density of the charge released during TSD is comparable to the domain density of both systems. Although parts of TSD spectra for these two systems were reported at several instances,^{4,21,22} our extensive measurements in various conditions provide a new insight into CDW freezing at finite temperature.

II. EXPERIMENTAL PROCEDURE

A. Theory of thermally stimulated depolarization

The procedure of thermally stimulated depolarization relies on the assumption that the polarization in the sample induced by an external electric field “freezes” on cooling to sufficiently low temperature, i.e., its relaxation time becomes far longer than the experimental time scale. The relaxation of polarization, or depolarization, is subsequently induced by heating without the field. The depolarization current spectra $j(T)$ are recorded and used to obtain the characteristics of the polarizing mechanisms and the corresponding dielectric properties. Essentially, the polarizing mechanisms may be divided in two basic groups: the dipole orientation and free carrier trapping. The basic difference between these two groups is that in the case of the dipole polarization the separation of charge is local and remains local, whereas in the case of free carrier trapping the separation of charge occurs at large distances, i.e., the opposite charges are usually trapped near the corresponding contacts.

Typically, the sample is cooled in external (poling) electric field E_{pol} from a high (poling) temperature T_{pol} to some low temperature T_{start} and, after removal of the field, heated using various heating schemes while the short-circuit depo-

larization current is measured. If the relaxation time of the induced polarization becomes comparable to the experimental time scale at some temperature, it will show up as a peak in the current spectrum at some temperature T_{max} . However, if the investigated sample is not a very good insulator, additional “background” current will be recorded due to either the voltage burden of the current meter or the contact potential, which might hinder the observation of the TSD current. Several parameters, such as T_{pol} , E_{pol} , or the heating rate h may be varied, which enables the distinction of different processes, deduction of polarizing mechanisms, estimation of the static dielectric constant ϵ , and the characteristic relaxation time τ , as well as the nature and parameters of the distribution of microscopic processes.

Data analysis is usually based on theoretical results obtained for a simple dipolar (Debye) system of noninteracting dipoles with a constant microscopic dipole moment p_0 and the activated temperature dependence of relaxation times,

$$\tau(T) = \tau_0 \exp(E_{act}/T). \quad (1)$$

It also represents the oversimplified limit of the carrier trap model. The deviations from this simple model, such as complex carrier trap mechanisms, distributions of microscopic parameters (p_0 , τ_0 , and E_{act}), or a different temperature dependence of τ , are usually clearly seen in the results and in some instances may be even quantified.

In the Debye model the decay rate is proportional to the polarization itself $dP/dt = P/\tau$, where τ is the relaxation time. As the depolarization current density j is a measure of the polarization (P) decay in time $j(t) = d(P(t))/dt$, for the constant $h = dT/dt$, the result is $j(T) = hP(T)/\tau(T)$. Thus for low temperatures where $P(T)$ is still rather constant $j(T)$ should have the same activated temperature dependence as $\tau(T)$. This is used as the initial step in the analysis to obtain the effective activation energy E_{eff} from

$$E_{eff} = \left. \frac{d(\log(j(T)))}{d(1/T)} \right|_{T \approx T_{start}}. \quad (2)$$

This E_{eff} corresponds to E_{act} only when τ is the same for all microscopic dipoles which is rarely the case. A more accurate estimate of E_{act} results from the variation of the heating rate h . For the Debye model the peak in the current spectrum occurs at the temperature where $d(\tau(T))/dT = -1/h$ which transforms to

$$\tau(T_{max}) = T_{max}^2 / (E_{act} h). \quad (3)$$

This equation may be used to estimate τ_{eff} for any peak in the current spectra from the known values of T_{max} , h , and E_{eff} . Varying h , the $\tau_{eff}(T)$ dependence may be obtained and fitted to Eq. (1) in order to find E_{act} which is not sensitive to the possible distribution of microscopic parameters. This value may then be used to recalculate τ_{eff} (which does not affect the value of E_{act}). Moreover, for a range of distributions in which the tails fall off exponentially or faster, the distribution width may be obtained as $w = E_{act}/E_{eff}$. However, $\tau_{eff}(T)$ might not depend on h at all, in which case the polarization may be assigned to carrier trapping.

Temperature dependent polarization $P(T)$ may be reconstructed by integrating $j(T)$ in temperature as

$$P(T) = \int_{T_{\text{start}}}^{T_{\text{stop}}} j(T') dT' / h. \quad (4)$$

The low temperature value of $P(T)$ provides information on the overall released charge per area P_0 and may be used to calculate the dielectric constant (or polarizability) as

$$\epsilon = P_0 / E_{\text{pol}}. \quad (5)$$

By varying E_{pol} a possible nonlinear dependence of ϵ may be deduced. For dipoles, ϵ is typically constant at low fields and decreases (P_0 saturates) at high fields, while for charge trapping ϵ may first increase at low fields. Also, P_0 should remain constant in the variation of h for dipole polarization, while for charge trapping it may increase for high h .

$\tau(T)$ may also be obtained directly from $\tau(T) = hP(T)/j(T)$, but again only if there is the unique τ for all microscopic processes. Otherwise, it will produce the same E_{eff} as obtained from the initial current rise analysis.

Another method which helps to distinguish different processes and different distributions is the partial depolarization in which the sample polarized at high T_{pol} is sequentially heated to and cooled from higher and higher “stop” temperatures $T_{\text{stop}} < T_{\text{pol}}$ without applying an of electric field. This way, the fraction of processes below T_{stop} is already relaxed and the “local” E_{eff} near T_{stop} may be obtained. The nonmonotonous dependence of E_{eff} (T_{stop}) may point to the existence of overlapping processes. Moreover, for a distribution in $\tau_0 E_{\text{eff}}$ will saturate to the value close to E_{act} below T_{max} of the full spectrum, while for the distribution in E_{act} it will smoothly increase up to T_{max} and will not reach E_{act} obtained from h variation.

Finally, the comparison with the expression for the dielectric response of the Debye model allows for an approximate calculation of the temperature-dependent imaginary part of the dielectric function from the TSD current spectrum as

$$\epsilon''(T) = 1.36j(T) \frac{T^2}{hE_{\text{act}}E_{\text{pol}}}. \quad (6)$$

This relation is strictly true at T_{max} and for a wider temperature range a variation of E_{act} with temperature might be important.

From the analysis presented above it is evident that the thermally stimulated depolarization method represents a viable alternative to dielectric spectroscopy in highly resistive and polarizable systems as it may provide the basic parameters of slow dielectric relaxation processes. Moreover, complementary information on the nature of relaxation processes and the distributions of parameters may be obtained as well, so, depending on the goals of the research it may even be a more suitable method. We believe that our results support both of these hypotheses.

B. Experimental details

The TSD current was measured in two experimental setups. The first one is appropriate for currents above 10^{-13} A

and uses the Keithley 617 electrometer for current measurements and as the voltage source. The second one is appropriate for currents as low as 10^{-15} A but with the high current limit of 5×10^{-12} A using a custom-made current meter and voltage source. Typically, the first setup allowed measurements only down to 10 K, while the second allowed measurements down to liquid helium temperatures.

In our measurements T_{pol} was selected to be about two times higher than the temperature at which the freezing of various processes was observed in dielectric spectroscopy.^{3,4} Both E_{pol} and h were varied for at least two orders of magnitude and we performed the partial depolarization as well. We varied E_{pol} in order to study the effect of a well-known strong variation of CDW conductivity with an applied electric field on TSD spectra. The variation of h samples different effective relaxation times and partial depolarization allows the investigation of the distribution of relaxation processes as well as the distribution of microscopic parameters.

Non-negligible contribution from the background current due to the finite conductivity of samples had to be subtracted from experimental data in order to extract the TSD current. Fortunately, this background was reproducible throughout our measurements, which was verified several times. Approximate temperature dependence of the background current has been $I_{\text{bg}} = I_0 \exp(-E_0/T)$ with $I_0 = 2.2 \times 10^{-3}$ A and $E_0 = 470$ K between 15 and 50 K for $\text{K}_{0.3}\text{MoO}_3$ and $I_0 = 6.3 \times 10^{-6}$ A and $E_0 = 520$ K between 20 and 60 K for o-TaS₃. Below these temperature ranges I_{bg} was of the order of the noise level. I_{bg} also restricted the quality of the TSD spectra for low applied electric fields.

Three samples of $\text{K}_{0.3}\text{MoO}_3$ and five samples of o-TaS₃ were used for measurements in two-contact configuration. Both the CDW transition temperature and the activated temperature dependence of the conductivity below T_p showed good agreement with standard four-contact measurements performed on samples from the same batches, demonstrating that the contact resistance becomes negligible below T_p . Some quantitative difference was observed between the TSD spectra of different samples, mostly for $\text{K}_{0.3}\text{MoO}_3$, but the qualitative features remain the same. The results are presented for a single sample of $\text{K}_{0.3}\text{MoO}_3$, on which all procedures were applied and for three o-TaS₃ samples. The dimensions of the $\text{K}_{0.3}\text{MoO}_3$ sample were $l = 0.7$ cm, $S = 0.7$ mm², and of the o-TaS₃ samples were (I) $l = 0.42$ cm, $S = 250$ μm^2 , (II) $l = 0.27$ cm, $S = 360$ μm^2 , and (III) $l = 2.2$ cm, $S = 630$ μm^2 .

III. RESULTS

Figure 2 presents typical TSD spectra for $\text{K}_{0.3}\text{MoO}_3$ and o-TaS₃ (sample I). These spectra were obtained in the saturation regime with the applied E_{pol} much higher^{23,24} than E_T at T_{pol} . Two peaks were observed for each system, signifying the freezing of the slow relaxation processes at corresponding temperatures. In line with dielectric spectroscopy we named the high temperature peak α and the low temperature peak β . For $\text{K}_{0.3}\text{MoO}_3$ the β peak appears more as an extra low temperature shoulder of the α peak and may be dis-

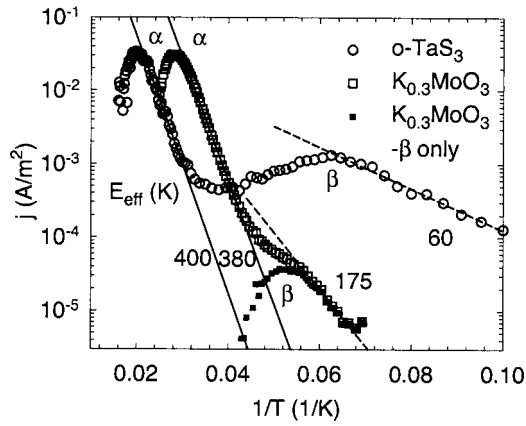


FIG. 2. The characteristic TSD spectra of $K_{0.3}MoO_3$ and $o-TaS_3$. For $K_{0.3}MoO_3$ $T_{pol}=50$ K, $h=11$ K/min, and $E_{pol}=1.4$ V/cm, while for $o-TaS_3$ $T_{pol}=70$ K, $h=14$ K/min, and $E_{pol}=240$ V/cm. For both systems E_{pol} is far above E_T at T_{pol} . Straight lines represent fits to the activated increase of $j(T)$. The β peak in $K_{0.3}MoO_3$ was obtained after the subtraction of the activated fit of the α process $j(T)$ from experimental data.

cerned as a peak only after the subtraction of the low temperature wing of the α process. The peak currents I_{max} of the α process are 2.2×10^{-8} A for $K_{0.3}MoO_3$ and 1.3×10^{-11} A for $o-TaS_3$. However, current densities for the α peak are very similar for two systems despite the difference of more than three orders of magnitude in sample cross-sections.

Various parameters extracted directly from the presented spectra or calculated according to the analysis presented in the previous section are given in Table I, together with the parameters obtained from dielectric spectroscopy.^{3,4} The comparison is quite favorable for the case of $o-TaS_3$, while for $K_{0.3}MoO_3$ the values from TSD are systematically higher than in dielectric spectroscopy. However, it was shown that both dc bias⁶ and increased signal amplitude²⁵ in dielectric spectroscopy of CDW systems increase $\Delta\epsilon$ and τ , therefore it is not surprising that the α process freezes at higher temperatures and has a higher polarizability in the saturated regime. The only parameter which is lower in TSD for both systems is the E_{act} , reflecting the distribution of microscopic relaxation processes, as already demonstrated in dielectric spectroscopy. We will discuss these results in more detail later, when full sets of data for various procedures are presented.

We also roughly calculated the $\epsilon''(T)$ from Eq. (6) for both systems and we present it in Fig. 3 together with the results of dielectric spectroscopy for several frequencies.^{3,4} The TSD results, which correspond to a very low frequency compared to dielectric data, seem a reasonable extrapolation, however, with substantially higher amplitudes for the α process.

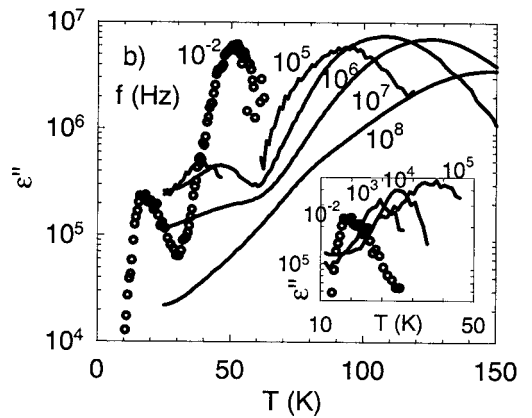
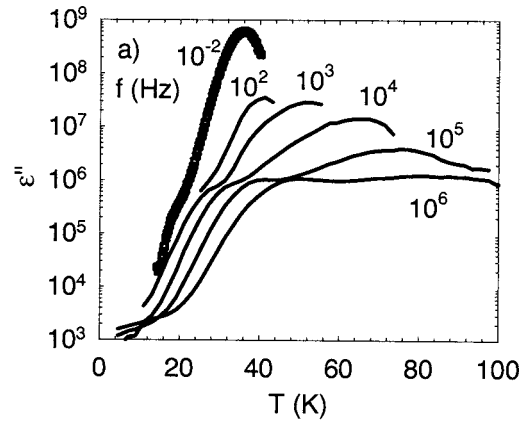


FIG. 3. Effective $\epsilon''(T)$ calculated from the TSD spectra in Fig. 2 compared to the directly measured (Refs. 3 and 4) $\epsilon''(T)$ for (a) $K_{0.3}MoO_3$ and (b) $o-TaS_3$ at several frequencies between 10^8 and 10^2 Hz. For TSD the effective frequency is calculated as $1/(2\pi\tau_{eff})$ with τ_{eff} for α from Table I. For $o-TaS_3$ the α process is presented in the main panel and the β process in the inset for clarity.

Even this rough analysis for a single TSD current spectrum for each system demonstrates that TSD is a viable alternative to dielectric spectroscopy for the study of very slow relaxation processes. In the following subsections we will discuss the results obtained for different TSD procedures we have applied in more detail, which also allowed the extraction of some additional information about relaxational processes.

A. Thermally stimulated depolarization in $K_{0.3}MoO_3$

The TSD current spectra of $K_{0.3}MoO_3$ obtained in different conditions are presented in Figs. 4–6. Maximum E_{pol} was restricted by the Joule heating and the maximum h by the temperature lag between the sample and the thermometer. Low-temperature/current data emerged from the noise level

TABLE I. Effective dielectric data obtained from the TSD spectrum in Fig. 2 and the corresponding dielectric spectroscopy data.

System	Peak/process	T_{max} (K)	E_{eff}	τ_{eff} (s)	$\Delta\epsilon_{eff}$	T_g (K)	E_{act} (K)	$\Delta\epsilon(\sim T_g)$
$K_{0.3}MoO_3$	α	36	380	29	1.1×10^9	23	635	6×10^7
$K_{0.3}MoO_3$	β	19	175	20	9×10^5	13	325	3×10^5
$o-TaS_3$	α	50	400	27	9×10^6	42	770	3×10^6
$o-TaS_3$	β	16	60	18	2×10^5	13	300	10^7

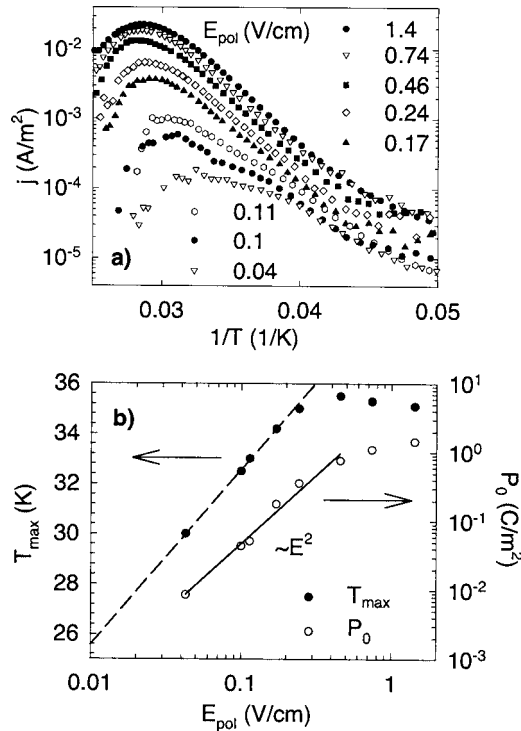


FIG. 4. (a) The TSD current spectra of $K_{0.3}MoO_3$ obtained for various E_{pol} with $T_{pol}=50$ K and $h=7$ K/min. (b) P_0 and T_{max} as the function of E_{pol} extracted from the TSD current spectra in Fig. 4(a). The full line indicates the quadratic E_{pol} dependence and the dashed line provides the extrapolation of T_{max} to low poling fields.

below 20 K only for the highest poling voltage [as seen in Fig. 4(a)], so the E_{pol} variation for the β process could not be studied. For other, smaller $K_{0.3}MoO_3$ samples the TSD current was even smaller and well inside the noise level below 20 K for any E_{pol} . Low-temperature/current data in partial depolarization (Fig. 6) were obtained with the custom-made current meter specially designed for very low currents.

Figure 4(a) evidently shows that both the peak position of the TSD current spectra and its value depend strongly on E_{pol} , as observed previously.^{4,21} The E_{pol} dependence of T_{max} and P_0 for the α process is presented in Fig. 5(a). At low E_{pol} P_0 increases almost quadratically and then saturates above app. 200 mV/cm, which is the value of E_T at 50 K, i.e., T_{pol} . The corresponding effective ϵ_0 calculated from Eq. (5) therefore increases linearly up to an extreme value of 1.4×10^9 at E_T and then starts to decrease slowly. T_{max} shown in Fig. 4(a) also increases with E_{pol} up to 200 mV/cm and then saturates above, while on the other hand E_{eff} obtained from the initial current rise remains fairly constant and of the order of 380 K. This clearly reflects strong dependence of the CDW response on the electric field, as expected from dielectric measurements.^{6,25} It is particularly important in $K_{0.3}MoO_3$ for which E_T decreases strongly with temperature from a few 100 mV/cm below T_p down to a few mV/cm at 10 K. Therefore, in order to compare effective dielectric data obtained from TSD, the extrapolation to low E_{pol} of about 10 mV/cm, the typical excitation field in dielectric measurements, should be made. This gives ϵ_0 of the order of 10^8 , T_g below 26 K, and the effective relaxation time $\tau_{eff}=22$ s calculated from Eq. (3), in a much better agreement with the dielectric data in Table I.

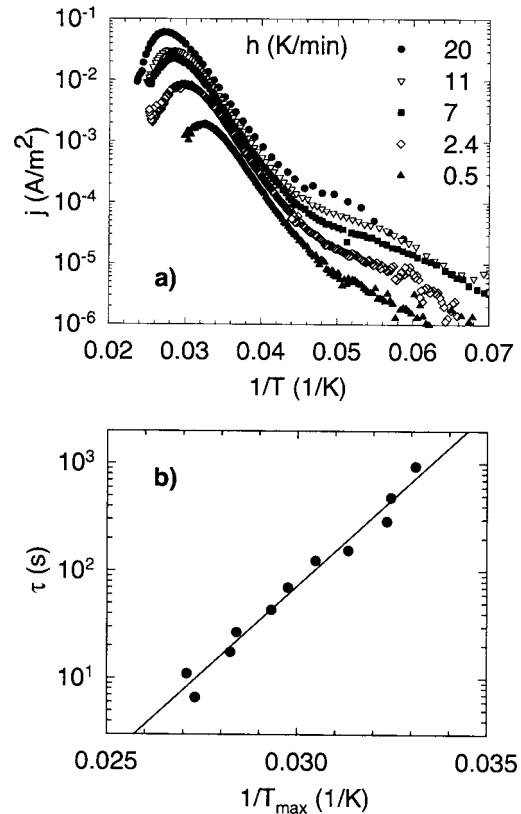


FIG. 5. (a) The TSD current spectra of $K_{0.3}MoO_3$ obtained for various h with $T_{pol}=50$ K and $E_{pol}=1.4$ V/cm. (b) τ_{eff} as the function of T_{max} for different h as extracted from the TSD current spectra of $K_{0.3}MoO_3$ in Fig. 5(a). The line indicates activated T_{max} dependence with $E_{act}=700$ K and $\tau_0=10^{-8}$ s.

The overall released charge in saturation amounts to one electron per 8×10^{-16} cm³, while in the low field limit it is one electron per app. 8×10^{-14} cm³. The later value is very close to the average phase domain volume of 7×10^{-14} cm³ estimated from x-ray diffraction,¹⁴ explicitly confirming the freezing criterion we have suggested based on low field dielectric measurements,⁴ as discussed in the Introduction.

The h dependence of the TSD current spectra was studied in highest E_{pol} in order to enable the measurement of the current spectra at very low heating rates. This dependence is very similar to the canonical case of the thermally activated independent dipoles. As evident in Fig. 5(a), the spectral shape does not change noticeably with h nor does $P_0 = 1.4$ C/m². On the other hand, T_{max} increases monotonously with h , facilitating the extraction of the temperature dependence of the effective relaxation time τ_{eff} calculated from Eq. (3) and presented in Fig. 5(b). $\tau_{eff}(T)$ increases in the activated manner over two decades and gives the distribution-independent activation energy of $E_{act}=700$ K, which is very close to E_{act} obtained from $\tau(T)$ in dielectric measurements. The microscopic relaxation time is $\tau_0=10^{-8}$ s. The ratio of E_{eff} from $j(T)$ to E_{act} from the heating rate dependence is $w=2.3$ indicating a broad distribution of relaxation parameters, much broader than in dielectric spectroscopy⁴ where $w=1.6$.

For the given τ_{eff} , even if recalculated with E_{act} , the freezing temperatures are still quite high compared those ob-

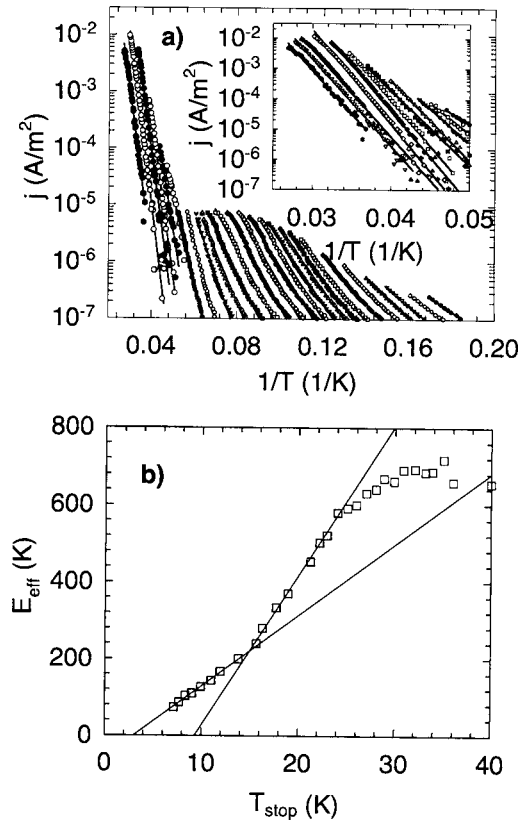


FIG. 6. (a) This TSD current spectra of $K_{0.3}MoO_3$ obtained for partial depolarization with $T_{pol}=50$ K, $E_{pol}=1.4$ V/cm, and $h=7$ K/min. (b) E_{eff} as the function of T_{stop} in partial polarization as extracted from the TSD current spectra of $K_{0.3}MoO_3$ in Fig. 6(a).

tained from the dielectric response,⁴ which would be actually expected^{6,25} for $E_{pol} \gg E_T$. Also from Fig. 4 it is obvious that for a comparison with small signal measurements the temperatures should be rescaled to substantially lower values which would produce a better agreement.

A small shoulder below 20 K in Fig. 5(a) indicates the secondary peak related to the β process observed in dielectric spectroscopy. The ratio of the maximum current of α peak and the current at the low-T shoulder is about 10^3 , as compared to the 10^2 ratio of α and β processes in Ref. 4. However, in $K_{0.3}MoO_3$ below about 20 K the high temperature nonlinear regime disappears and a new one²⁶ sets in with a very high E_T of about 10 V/cm. In this respect, we are well above the (high temperature) linear regime for the α process, but well within the (low temperature) linear regime for the β process, so we expect that at low E_{pol} this ratio should approach 10^2 .

Partial depolarization spectra in Fig. 6(a) are obtained from two runs on the same sample under the same conditions, but with the current measured with different devices applicable for the corresponding current ranges. However, the resulting spectra are very close in the overlap region. E_{eff} in Fig. 6(b) obtained from the $j(T)$ slope in Fig. 6(a) depends strongly on T_{stop} , signifying distributed processes. Moreover, the crossover around 16 K shows that the contributions below and above this temperature come from different processes, which is in agreement with the existence of the α and β processes. E_{eff} for the β process increases all the way up to

the temperature of the maximum in full TSD spectra at 19 K. On the other hand, E_{eff} for the α process saturates to the cutoff value of about 700 K (in agreement with the h variation results) above 30 K, which is lower than T_{max} in the full spectrum. This indicates that the distribution of microscopic parameters of the β process is in the activation energy E_{act} , while for the α process it is in the relaxation time τ_0 .

B. Thermally stimulated depolarization in o-TaS₃

The TSD current spectra of the α process in o-TaS₃, such as presented in Fig. 2, could be obtained only for the highest E_{pol} and h as even in this case the TSD current at T_{max} was only about 10% of the background current. In this respect, all available data on the α process are already presented in Table I. However, we may estimate the released charge corresponding to the α process which amounts to one electron per 3×10^{-16} cm³. This is again in agreement with the estimates of the average phase domain volume of 1.2×10^{-16} cm³ obtained by the dark field electron microscopy,¹³ and also confirming the freezing criterion we have suggested based on dielectric measurements³ for o-TaS₃. Unlike in $K_{0.3}MoO_3$, the effect of the increased released charge for $E_{pol} \gg E_T$ is substantially reduced due to the exponential increase of E_T at low temperatures,²⁷ which is of the order of 100 V/cm near $T_{max}=50$ K, thus comparable with E_{pol} .

In this subsection we present therefore the results obtained in different conditions only for the low temperature β peak. With whiskerlike samples the TSD currents were substantially lower than in $K_{0.3}MoO_3$, so only a low current device have been used. The TSD current spectra of o-TaS₃ obtained in different conditions are presented in Figs. 7–9.

Figure 7 shows the TSD current spectra obtained for different E_{pol} . They present two distinct phenomena, a narrow peak situated at $T_{max}=16$ K and a low temperature tail below app. 12 K, suggesting two polarizing mechanisms. This may be related to the existence of yet another very low temperature process β_0 observed³ in o-TaS₃. Only for the highest fields do these two regimes merge to produce a very wide peak. E_{eff} obtained from $j(T)$ is 20 K below 12 and 200 K above 12 K for the lowest E_{pol} . As E_{pol} increases the overlap of the peak and the low temperature tail smears these two regimes and at the highest E_{pol} $E_{eff}=30$ K in the entire temperature range below the maximum. τ_{eff} is about 200 s. The overall released polarization P_0 is presented in Fig. 7(b) as a function of E_{pol} together with the polarization released up to 12 K ($P_{12 K}$). While P_0 , due mostly to the TSD current in the peak region, increases linearly up to 10 V/cm and then saturates, $P_{12 K}$ remains linear for all E_{pol} , which is the reason for the overlap of the two contributions for the highest E_{pol} .

The corresponding effective ϵ_0 calculated from P_0 as in Eq. (5) has a high value of 1.4×10^7 at low E_{pol} which compares favorably with the low field dielectric spectroscopy data in Table I. For higher E_{pol} it decreases due to the saturation for more than one order of magnitude. This type of E_{pol} dependence is quite similar to independent dipoles apart from the much smaller saturation offset field which is of the

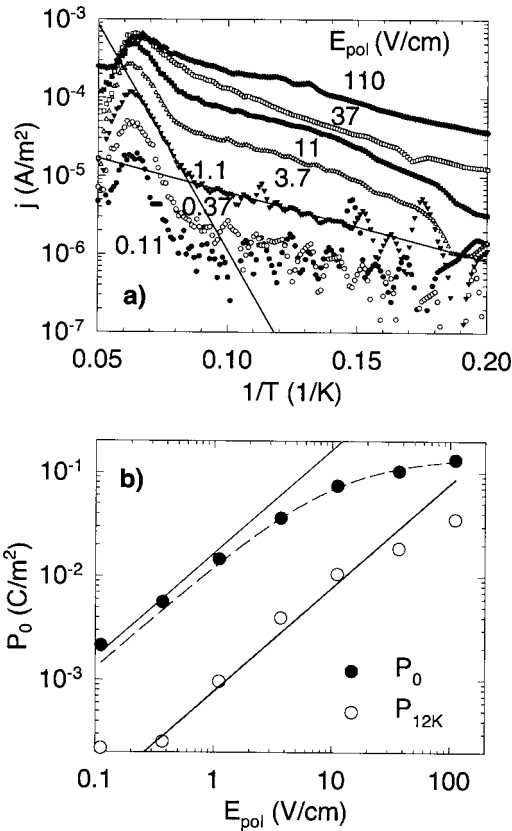


FIG. 7. (a) The TSD current spectra of o-TaS₃ obtained on sample II for various E_{pol} with $T_{\text{pol}}=30$ K and $h=2$ K/min. Straight lines are fits to the activated temperature dependence above and below 12 K. (b) P_0 and $P_{12\text{K}}$ as the function of E_{pol} as extracted from the TSD spectra in Fig. 7(a). Straight lines indicate linear E_{pol} dependence, while the dashed line is the guide to the eye corresponding to the saturation of P_0 at high E_{pol} .

order of MV/cm for ordinary dipolar materials. Effective ϵ_0 obtained from $P_{12\text{K}}$ is about 7×10^5 , which is a few times smaller, but still of the order of magnitude of the β_0 process.³ However, $P_{12\text{K}}$ evidently does not correspond with the entire charge released through this very low temperature depolarization process as it overlaps with the peak at 16 K, so this ϵ_0 is underestimated.

The h dependence presented in Fig. 8(a) was studied in the highest E_{pol} , so very low currents at low h could be measured. The spectra shapes are quite similar for different h , and so is $P_0=6 \times 10^{-2}$ C/m². In Fig. 8(b) the dependence of τ_{eff} , calculated as in Eq. (3), is presented as the function of T_{max} for different h . The activated dependence over two decades gives $\tau_0=7 \times 10^{-10}$ s and $E_{\text{act}}=420$ K, which is again very close to E_{act} obtained from $\tau(T)$ in dielectric spectroscopy. The ratio of E_{eff} from $j(T)$ in the peak region to E_{act} from heating rate dependence is $w=2$ indicating a broad distribution of relaxation parameters, in agreement with dielectric spectroscopy results.³

Partial depolarization spectra are presented in Fig. 9(a). E_{eff} in Fig. 9(b) obtained from the $j(T)$ slope in Fig. 9(a) depends strongly on T_{stop} , again signifying distributed processes. E_{eff} increases monotonously all the way up to T_{max} obtained in full TSD spectrum and then saturates to about 300 K, which is substantially lower than E_{act} obtained from h

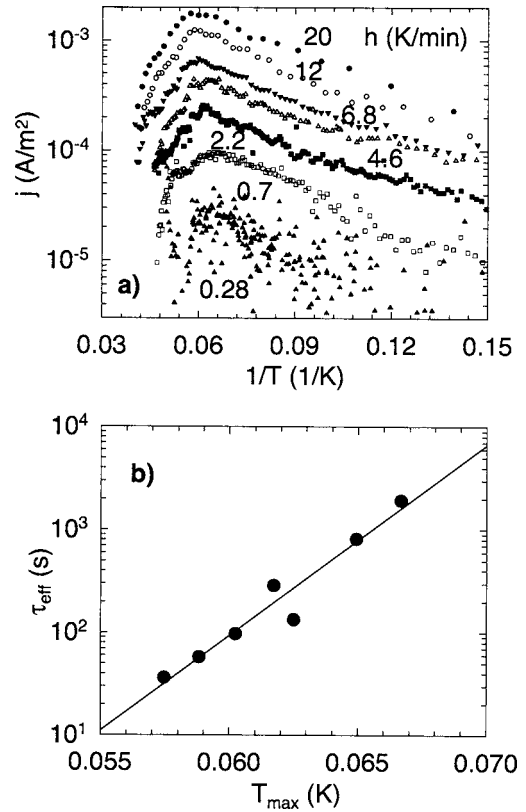


FIG. 8. (a) The TSD current spectra of o-TaS₃ obtained on sample III for various h with $T_{\text{pol}}=30$ K and $E_{\text{pol}}=45$ V/cm. (b) τ_{eff} as the function of T_{max} for different h extracted from the TSD spectra in Fig. 8(a). The line indicates the activated T_{max} dependence with $E_{\text{act}}=420$ K and $\tau_0=7 \times 10^{-10}$ s.

variation. Just as for the β process in $\text{K}_{0.3}\text{MoO}_3$, it indicates that the distribution of parameters of the β process in o-TaS₃ is in E_{act} as well.

IV. DISCUSSION

The measurements of the thermally stimulated depolarization current spectra in two canonical charge density wave systems o-TaS₃ and $\text{K}_{0.3}\text{MoO}_3$ provided direct evidence of the existence of two slow relaxation processes in each system which freeze at finite temperatures. Dielectric properties calculated from the TSD spectra are in good agreement with the results of the dielectric spectroscopy. We were able to relate the high temperature α and the low temperature β processes from TSD and dielectric spectroscopy in both systems. Moreover, the charge released under the α peak in the TSD spectra of both systems corresponds quite closely to the spatial density of one electron per CDW phase coherence domain. In our opinion, this is direct evidence that the freezing of the α process in a CDW system is a consequence of the Coulomb interaction of distorted CDW which freezes the domain dynamics in the absence of free carrier screening, as we proposed previously.^{3,4}

There are several features that distinguish the TSD spectra of the α process obtained in CDW systems from typical TSD spectra obtained either for dipolar or trapping mechanisms. On the other hand, the independence of the released charge on the heating rate signifies that no fast carrier recombination process takes place and points to the dipolar origin

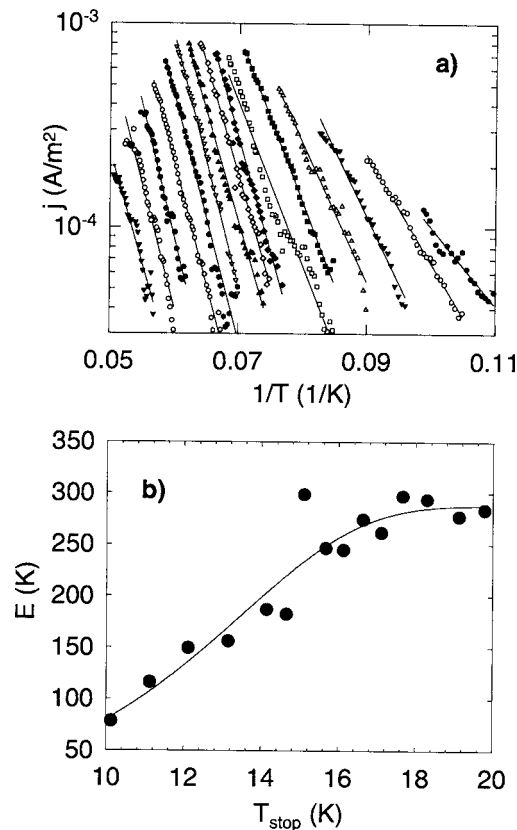


FIG. 9. (a) The TSD current spectra of o-TaS₃ obtained on sample III for partial depolarization with $T_{\text{pol}}=30$ K, $h=10$ K/min, and $E_{\text{pol}}=45$ V/cm. (b) E_{eff} as a function of T_{stop} in partial polarization extracted from the TSD spectra in Fig. 9(a).

of the TSD spectra. On the other hand, strong dependence of both P_0 and T_{max} on E_{pol} points to the space charge polarization. This discrepancy, however, might be reconciled in the case of CDW systems. The low energy excitations in CDW systems arise from interaction with random impurities which break a CDW in the domains of correlated phase separated by domain walls in which the phase is spatially distorted. As the spatial distortion of the CDW phase results in local charge excess, these domains may be roughly considered as dipoles.¹⁶ In the absence of free carriers the domains are frozen due to a strong electrostatic interaction¹⁵ and have no internal degrees of freedom. At higher temperatures the free carriers excited across the CDW gap screen the phase distortions to some extent and the domains acquire some highly constrained internal degrees of freedom resulting in overdamped, distributed low frequency relaxation.^{16–19} The charge released under the α peak corresponds quite closely to the number of phase domains, but also to the number of free carriers at T_{max} estimated from RT density and the activated temperature dependence of conductivity.^{3,4} In this respect the frozen domains, or more precisely the corresponding phase distortions, act as carrier traps similarly as in doped semiconductors. Also, the limiting, highest energy barrier obtained in TSD is again very close to the E_{act} (CDW gap) obtained from the semiconducting temperature dependence of conductivity, signifying that the relevant energy scale for the domain relaxation is the energy of free carrier excitation over the CDW gap.

While the general features of the TSD spectra and the corresponding parameters obtained in various conditions are rather similar for the two CDW systems presented here, there is one essential difference. Both $\Delta\epsilon$ and $j_{\text{max}}(\alpha)$ in K_{0.3}MoO₃ and o-TaS₃ are very similar. However, the β peak/process in K_{0.3}MoO₃ is more than one order of magnitude smaller than that in o-TaS₃. One may also relate it to the temperature dependence of E_T in these two systems, where E_T of o-TaS₃ increases exponentially at low temperatures, while for K_{0.3}MoO₃ it decreases strongly to very low values. It is just another manifestation of the same phenomenon. The data on the excess heat capacity due to the low energy excitations,²⁸ where this contribution in o-TaS₃ is shown to be almost two orders of magnitude larger than in K_{0.3}MoO₃, at least demonstrate that the number of phase defects in o-TaS₃ is substantially larger. From this observation other experimental differences might eventually be explained if it were shown that the CDW properties change qualitatively with the number of phase defects. However, it remains a pertinent question of these two canonical CDW systems which the present study cannot answer.

In conclusion, extensive measurements of the thermally stimulated depolarization current spectra in two canonical charge density wave systems o-TaS₃ and K_{0.3}MoO₃ provided direct evidence of the freezing of the two relaxation processes at finite temperatures in each of these systems. For the high temperature α process its CDW origin was confirmed, as well as the previously proposed^{3,4} freezing mechanism of the CDW phase based on interplay of pinning and screening.

ACKNOWLEDGMENTS

We would like to thank the Croatian MSES Project No. 035-0352827-2842 for their support of this research, as well as Dr. P. Monceau for the suggestions and encouragement.

- H. Frölich, *Proc. R. Soc. London, Ser. A* **223**, 296 (1954); R. E. Peierls, *Quantum Theory of Solids* (Oxford University Press, London, 1955), p. 108; W. Kohn, *Phys. Rev. Lett.* **2**, 393 (1959).
- Electronic Properties of Inorganic Quasi-One-Dimensional Compounds*, edited by P. Monceau (Kluwer Academic, Dordrecht, 1985); G. Grüner, *Rev. Mod. Phys.* **60**, 1129 (1988); *Charge Density Waves in Solids*, edited by L. Gor'kov and G. Gruner (Elsevier Science, Amsterdam, 1989); G. Grüner, *Density Waves in Solids* (Addison-Wesley, New York, 1994).
- D. Starešinić, K. Biljaković, W. Brütting, K. Hosseini, P. Monceau, H. Berger, and F. Levy, *Phys. Rev. B* **65**, 165109 (2002).
- D. Starešinić, K. Hosseini, W. Brütting, K. Biljaković, E. Riedel, and S. van Smaalen, *Phys. Rev. B* **69**, 113102 (2004).
- P. G. Debenedetti and F. H. Stillinger, *Nature (London)* **410**, 259 (2001).
- R. J. Cava, R. M. Fleming, P. Littlewood, E. A. Rietman, L. F. Schneemeyer, and R. G. Dunn, *Phys. Rev. B* **30**, 3228 (1984).
- R. J. Cava, R. M. Fleming, R. G. Dunn, and E. A. Rietman, *Phys. Rev. B* **31**, 8325 (1985).
- R. J. Cava, P. Littlewood, R. M. Fleming, R. G. Dunn, and E. A. Rietman, *Phys. Rev. B* **33**, 2439 (1986).
- W. G. Lyons and J. R. Tucker, *Phys. Rev. B* **40**, 1720 (1989).
- F. Ya. Nad' and P. Monceau, *Solid State Commun.* **87**, 13 (1993); F. Nad' and P. Monceau, *Phys. Rev. B* **51**, 2052 (1995).
- C. A. Angell, *J. Non-Cryst. Solids* **131–133**, 13 (1991).
- H. Fukuyama and P. A. Lee, *Phys. Rev. B* **17**, 545 (1978).
- H. Chen and R. M. Fleming, *Solid State Commun.* **48**, 777 (1983).
- S. M. DeLand, G. Mozurkewich, and L. D. Chapman, *Phys. Rev. Lett.* **66**, 2026 (1991).
- A. Virosztek and K. Maki, *Phys. Rev. B* **48**, 1368 (1993).
- P. B. Littlewood, *Phys. Rev. B* **36**, 3108 (1987).
- S. N. Artemenko and A. F. Volkov, in *Charge Density Waves in Solids*,

- edited by L. Gor'kov and G. Grüner (North Holland, New York, 1989), p. 365.
- ¹⁸T. Baier and W. Wonneberger, *Z. Phys. B: Condens. Matter* **79**, 211 (1990).
- ¹⁹W. Aichmann and W. Wonneberger, *Z. Phys. B: Condens. Matter* **84**, 375 (1991).
- ²⁰J. van Turnhout, in *Electrets, Topics in Applied Physics*, edited by G. M. Sessler (Springer-Verlag, Berlin, 1985), Vol. 33, p. 81.
- ²¹R. J. Cava, R. M. Fleming, E. A. Rietman, R. G. Dunn, and L. F. Schneemeyer, *Phys. Rev. Lett.* **53**, 1677 (1984).
- ²²D. Starešinić, K. Biljaković, N. I. Baklanov, and S. V. Zaitsev-Zotov, *Synth. Met.* **103**, 2610 (1999).
- ²³G. Mihaly, P. Beauchene, J. Marcus, J. Dumas, and S. Schlenker, *Phys. Rev. B* **37**, 1047 (1988).
- ²⁴P. Monceau, H. Salva, and Z. Z. Wang, *J. Phys. (Paris), Colloq.* **44**, C3-1639 (1983).
- ²⁵R. J. Cava, R. M. Fleming, R. G. Dunn, E. A. Rietman, and L. F. Schneemeyer, *Phys. Rev. B* **30**, 7290 (1984).
- ²⁶A. Maeda, M. Notomi, and K. Uchinokura, *Phys. Rev. B* **42**, 3290 (1990).
- ²⁷M. E. Itkis, F. Ya. Nad, and P. Monceau, *J. Phys.: Condens. Matter* **2**, 8327 (1990).
- ²⁸K. Biljaković, *Phys. Rev. Lett.* **96**, 039603 (2006).